The Effect of Positional and Postural Errors When Attaching a Depth Camera to an Operating Light on Organ Tracking

Miho Asano[1], Satoshi Numata[2], Tsuneo Jozen[3], Hiroshi Nobori[4,*], Kaoru Watanabe[4], and Masanao Koeda[5]

[1] Department of Management and Data Business, Kobe University of Future Health Sciences, Osaka, Japan
[2] Department of Digital Games, Osaka Electro-Communication University, Osaka, Japan
[3] Department of Spatial Design, Osaka Electro-Communication University, Osaka, Japan
[4] Department of Computer Science, Osaka Electro-Communication University, Osaka, Japan
[5] Department of Human Information Engineering, Okayama Prefectural University, Okayama, Japan
Email: asano617@gmail.com (M.A.); numata@osakac.ac.jp (S.N.); jozen@osakac.ac.jp (T.J.); nobori@osakac.ac.jp (H.N.); kaoru@osakac.ac.jp (K.W.); koeda@ss.oka-pu.ac.jp (M.K.)
*Corresponding author

***Abstract*—In this study, we compared the tracking system of the liver in real space and virtual space by shifting the coordinates of the virtual camera and the actual camera, changing the shooting conditions, and changing the state of the liver incision. If we can determine which condition provides better tracking accuracy, our navigation system for outpatient surgery will be closer to completion. In this study, an accurate liver model was placed on a moving table and moved in parallel and up and down. The liver model in the virtual environment was tracked to evaluate its tracking system. In addition, since it is not always possible to set up a camera at the exact location when preparing for the surgery, we evaluated the tracking system by shifting the virtual camera coordinates and taking pictures.**

***Keywords*—real liver model, virtual liver model, fastest descent method, liver navigation, virtual camera**

I. Introduction

Surgical navigation is attracting a great deal of attention in fields such as orthopedic surgery, plastic surgery, neurosurgery, renal surgery and liver surgery.

Until now, most research has been focused on navigation in orthopedic surgery [1]. In comparison, surgical navigation in plastic surgery is relatively easy to construct because the main target is bone, and its structure and kinematics are geometrically fixed [2]. Also, because the brain is completely covered by the skull, this brain navigation is stable even if the brain itself is slightly deformed. Neuro-navigation is an area of research that is still developing [3], and currently, commercial surgical navigation systems such as the Stealth Station™ (provided by Medtronic Co.) are already in use.

However, there are no commercial liver navigation systems, and most of them are for research purposes. There are the following problems with liver navigation.

Manuscript received February 19, 2025; accepted August 11, 2025; published December 25, 2025.

There are two serious problems.

(1) Matching the real and virtual organs.

(2) Identifying the movement and deformation of the real organ.

In this study, we focus on problems (1). In this field, algorithms such as 3D stereo [4], Simultaneous Localization and Mapping (SLAM) [5–15], and Iterative Closest Point (ICP) of the Point Cloud Library (PCL) [16–24] are often used.

In this paper, we focus on Depth–Depth Matching (DDM), which can be easily used by simply attaching a depth camera to a location where the surgical site can be seen, such as a surgical light, and which has good computational efficiency for organ tracking [25–37]. In this study, we consider how much the superimposition accuracy changes when the position and posture of the virtual camera that controls the virtual liver and the real camera attached to the surgical light are misaligned and show that liver navigation can be used easily without camera calibration.

The DDM algorithm uses the difference between the depth images before and after the sampling time as an evaluation value and considers the direction in which the evaluation value is maximized in the 6-DOF space of translation and rotation as the actual direction of organ movement. Therefore, the higher the tracking accuracy, the more the surface shape of the organ changes in a direction that is orthogonal to the actual direction of movement. Therefore, the key to obtaining good tracking accuracy is to install the camera in advance so that the direction of movement of the organ during surgery is perpendicular to the incision shape change.

However, it is difficult to install such a camera during the hectic period before surgery. In this study, we evaluated the tracking accuracy from the virtual organ to the real organ in terms of the presence or absence of errors in the parallel and rotational components with respect to the optimal direction. As a result, we

doi: 10.18178/ijpmbs.14.4.129-136

experimentally showed that the parallel component error was completely irrelevant, and that the rotational component error did not need to be considered so much.

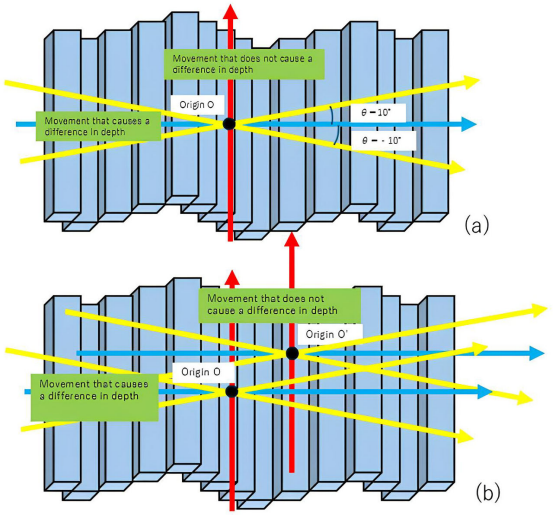

Fig. 1. (a) Rotational misalignment affects the change in depth difference. (b) Parallel misalignment does not affect the change in depth difference.

In Fig. 1(a), the aforementioned difference does not change fundamentally, no matter how much the real coordinates of the depth image and the virtual coordinates of the Z buffer are offset in the X or Y coordinate direction of the plane that is orthogonal to the image normal vector. Therefore, the parallel translation error component has no effect on the accuracy of the DDM algorithm when the depth camera is installed. However, in Fig. 1(b), if there is a deviation in the direction of rotation with respect to the Z-coordinate of the plane that is orthogonal to the image normal vector, the aforementioned difference will change, and this will affect the tracking accuracy. In this study, we verified the tracking accuracy in cases where there is no error in the direction of rotation and in case where there is an error of ±10°. As a result, it was found that there was almost no effect on the tracking accuracy with that degree of error.

Finally, in the case of the organ moving in the Y direction in Fig. 2, the difference before and after the sampling time of the depth image does not change at all, so it is not possible to extract the organ movement.

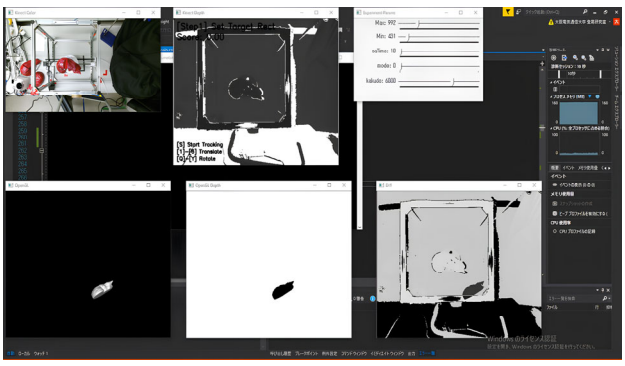

Fig. 2. Liver navigator window using the steepest descent method.

The structure of this paper is as follows. Section II describes the experimental environment. Section III describes the experimental results. Section IV discusses the experimental results. Section V summarizes this paper.

II. Experimental Methods and Equipment

In previous experiments, we studied the tracking accuracy of the liver under lighting conditions. We evaluated the accuracy of liver tracking under two different lighting conditions: a laboratory (fluorescent light, sunlight) and an operating room (halogen light). We found that the larger the cutting wound, the more accurately the virtual liver followed the real liver.

In this experiment, a real camera is installed in the operating theater's shadow lamp, and the virtual liver is made to follow the real liver based on the depth image. At this time, it is possible that the real camera cannot be installed in the same way as the virtual camera. Therefore, we will demonstrate that even if the coordinates of the virtual camera and the real camera do not match, the accuracy with which the virtual liver follows the real liver does not deteriorate significantly.

This chapter describes our experimental environment.

A. Liver-Tracking Navigator Based on the DDM-Based Gradient Descent Algorithm

This is the navigator used in this study. The initial alignment of the virtual space liver model and the real liver model is performed manually. The bottom right and top right middle windows in Fig. 2 show the depth images of the real liver model and the virtual space liver model, respectively, and the top right middle window also shows the matching rate between the virtual space model and the real space liver model. The area to be evaluated for the matching rate is specified by enclosing it as shown in Fig. 3. If you change the Max and Mix values in the top right window, only the liver model will be extracted cleanly from the top center window. Max specifies the position farthest from the camera within the image acquisition range, and Min specifies the closest distance within the image acquisition range. In the window in the lower left of Fig. 2, you can change the position of the liver model in the virtual space. You can rotate and translate along the X and Y axes and translate and rotate along the Z axis. These are used to synchronize the liver model in the virtual space with the real liver model. The time slider in the upper right window of Fig. 2 allows you to set the measurement time in one-second increments, and the Mode slider allows you to switch the search algorithm. Mode 1 allows for detailed alignment.

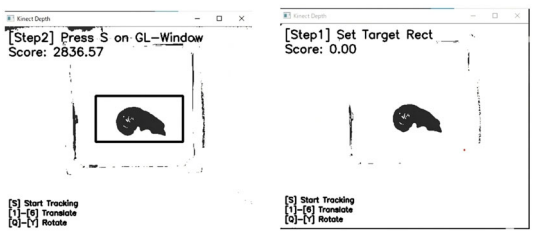

Fig. 3. Range specification and extracted window.

B. Equipment

In this study, the liver was tracked mainly under fluorescent lighting in a laboratory. As shown in Fig. 4, the liver was placed on a translational rotational motion measuring device and rotated to reflect a predetermined error. The liver was placed on the top of a bar and images of the liver were taken using the camera. The liver models used are shown in Fig. 5. These models are placed on the translational rotational motion measurement device, moving along the X and Y axes, rotating around the Z axis, and their images are taken by the camera.

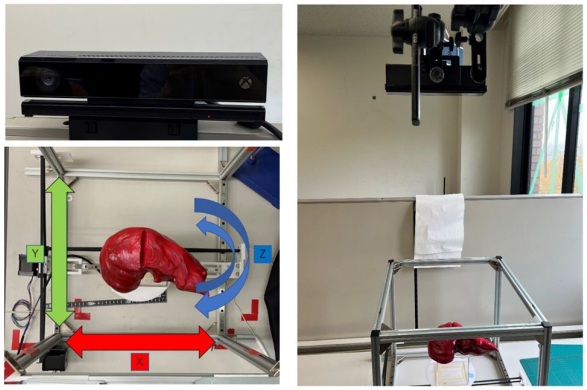

Fig. 4. Laboratory shooting environment. Parallel rotational movement measuring instrument and direction of operation.

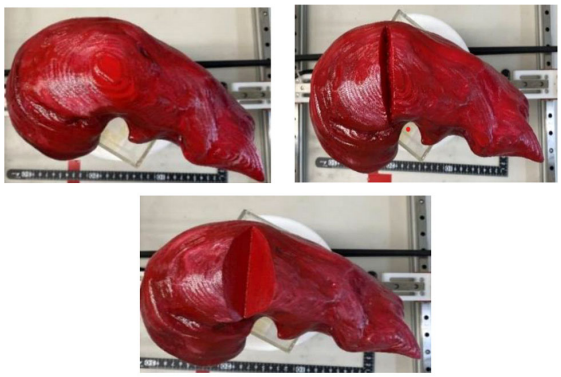

Fig. 5. (a) Liver model without resection, (b) slightly resected liver model, (c) largely resected liver model.

C. Camera Kinect v2

Kinect is a sensor device for the Xbox 360 home video game console, which was released by Microsoft in 2010. In 2021, Kinect for Windows was released. Kinect for Windows has an RGB camera and depth sensor built in. Kinect V2 was released by Microsoft in 2014. It is used to obtain data in depth.

D. Translation and Rotation Measurement Machine

The parallel translation and rotation measuring machine is used to improve the accuracy and reduce the error of the live navigator, which is the purpose of this research. The parallel translation and rotation measuring machine is a measuring machine consisting of three translation stages, which enables more accurate translation and angle measurement. Automatic translation is possible by sending commands to the parallel translation and rotation measuring machine using the GrblControl software. Figs. 4 and 5 show the parallel translation and rotation measuring machine.

E. Score

In the liver navigator that uses the steepest descent method, the degree of agreement between the real liver model and the liver model in the virtual space is expressed as a numerical value called a score. This score is calculated by comparing the images of the real liver model and the virtual liver model pixel by pixel, with the depth image of the real liver model being D_m and the depth image of the virtual liver model being D_s.

$$Score = \Sigma_{OR(Dm\ Ds)} |D_s - D_m|$$

It is defined and calculated. Based on D_s, D_m is calculated in pixel units. It shows how far D is from the standard. Next, all the calculated values are added up, squared and then the root is taken. The calculated value is used as the score.

III. Changing the Coordinate System of the Camera in the Virtual Space

In this experiment, we will shift the coordinates of the real camera and the camera into virtual space and acquire data. The intention of this experiment is to shift the coordinates of the camera in the real world and the camera in virtual space and acquire data, because it is not possible to position the camera appropriately in actual surgical operations. Assuming that it may not be possible to move the camera in the real world to the appropriate angle, the program changed the angle of the camera in the virtual space to −10 degrees on the X-axis and Y-axis, and +10 degrees on the Y-axis. The unit of angels is radians. The unit of angle is radians, and the calculation method is to input the base and angle, find the height, and calculate it as a virtual value. Since the principle of DDM is a difference calculation using linear projection, it is assumed to be strong against errors in the parallel component, so here we decided to add errors in the rotational component.

This value changes the angle of the camera in the virtual space. Figs. 6 and 7 are programs that change the angle of the camera in the virtual space by +10 to −10 degrees on each axis. Fig. 8 shows the camera coordinate system.

```
// View Setting
glMatrixMode(GL_MODELVIEW);
glLoadIdentity();
gluLookAt(0.0, 0.0, 0.0,     // 視点位置
    0.17632698070847, 0.0, 1.0, // 視点目標位置
    0.0, 1.0, 0.0); // 上方向ベクトル
```

```
// View Setting
glMatrixMode(GL_MODELVIEW);
glLoadIdentity();
gluLookAt(0.0, 0.0, 0.0,     // 視点位置
    -0.17632698070847, 0.0, 1.0,     // 視点目標位置
    0.0, 1.0, 0.0); // 上方向ベクトル
```

Fig. 6. (a) Program to change the angle of the camera in the virtual space by +10 degrees around the X axis, (b) Program to change the angle of the camera in the virtual space by −10 degrees around the X axis.

```
// View Setting
glMatrixMode(GL_MODELVIEW);
glLoadIdentity();
gluLookAt(0.0, 0.0, 0.0,     // 視点位置
    0.0, 0.17632698070847, 1.0, // 視点目標位置
    0.0, 1.0, 0.0); // 上方向ベクトル
```

```
// View Setting
glMatrix[illegible]MODELVIEW);
glLoadI[illegible]
gluLookAt(0.0, 0.0, 0.0,     // 視点位置
    0.0, -0.17632698070847, 1.0,     // 視点目標位置
    0.0, 1.0, 0.0); // 上方向ベクトル
```

Fig. 7. (a) Program to change the angle of the camera in the virtual space by +10 degrees around the Y axis, (b) Program to change the angle of the camera in the virtual space by −10 degrees around the Y axis.

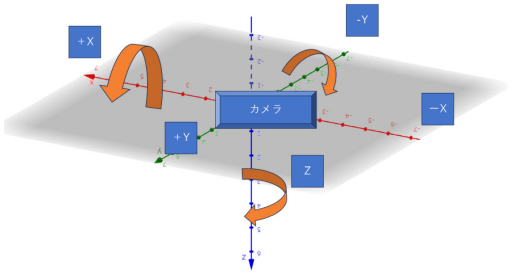

Fig. 8. Moving the camera in virtual space.

A. X-axis Rotation Errors

Fig. 9 shows a graph taken without moving the camera's coordinates in the virtual space. The higher the match rate, the greater the characteristics of the surgical wound. This indicates that the changes in the depth image are being captured well. In addition, the best match rate is around 300 (= 0.037 mm excludes a few millimeters of the Kinect v2's depth error), which indicates that the real and virtual organs are sufficiently superimposed [37].

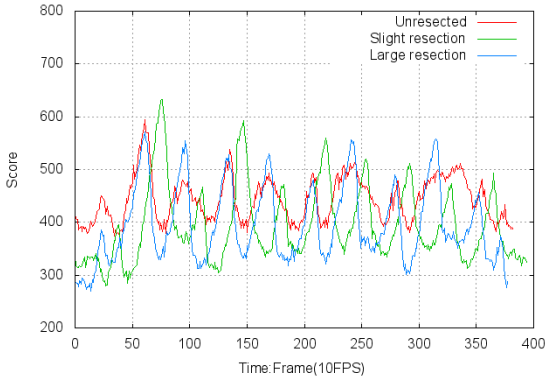

Fig. 9. The score changes when it moves back and forth ±30 mm in the X axis direction on the velocity 10 mm/sec.

1) Changing the camera coordinates in the virtual space angle around the X-axis +10 degrees, X-axis ±30 mm, 5 sets

The liver model was placed on the parallel rotation measuring device and moved at a speed of 30 mm/sec in the X-axis direction to evaluate the liver tracking accuracy. In addition, the camera in the virtual space was moved by +10 degrees around the X-axis to measure.

Firstly, tracking accuracy has improved significantly because of error. Secondly, the score improves in order of incision size. From the above, coordinate error and surgical wounds have a positive effect on organ tracking accuracy (Fig. 10).

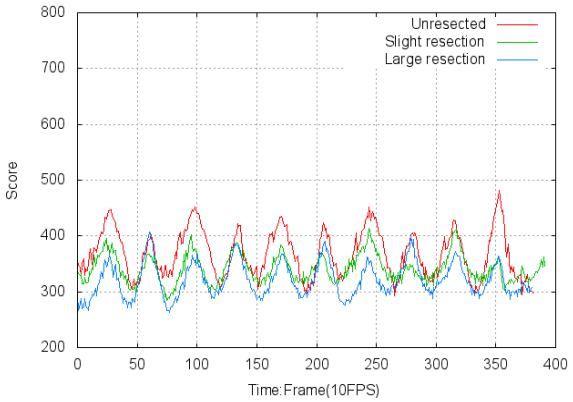

Fig. 10. When the virtual camera is rotated +10 degrees around the X axis relative to the real camera, the score changes when it moves back and forth ±30 mm in the X axis direction on the velocity 10 mm/sec.

2) Change in camera coordinates in virtual space angle around X-axis −10 degrees, X-axis ±30 mm, 5 sets

The camera in the virtual space was rotated 10 degrees counterclockwise around the X axis, and the same procedure as in Fig. 10 was used for the measurements (Fig. 11). Although not as good as in Fig. 10, the overall tracking accuracy was improved by the error, and in Fig. 11, the model with the liver resected scored well, showing the highest tracking accuracy.

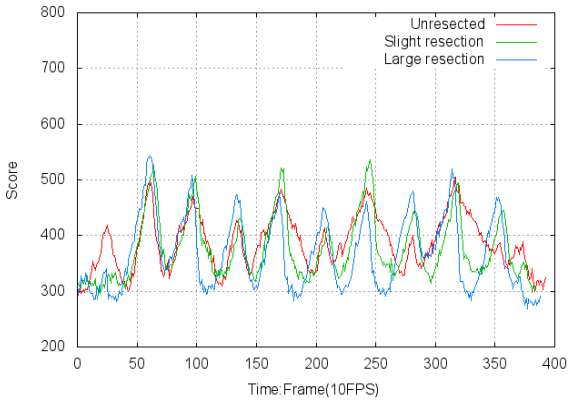

Fig. 11. When the virtual camera is rotated −10 degrees around the X axis relative to the real camera, the score changes when it moves back and forth ±30 mm in the X axis direction on the velocity 10 mm/sec.

3) Change in camera coordinates in virtual space angle around X-axis −10 degrees, Y-axis ±30 mm, 5 sets

The angle of the camera in the virtual space was changed by −10 degrees around the X-axis, and it was moved along the Y-axis at a speed of 30 mm per second according to the instructions of the parallel rotation motion measuring instrument, and the tracking accuracy of the liver was evaluated. The graph is shown in Fig. 12.

Compared to Figs. 10 and 11, the score values are generally higher, and the degree of agreement between the real liver model and the liver model in the virtual space is low. In addition, the score values fluctuate widely.

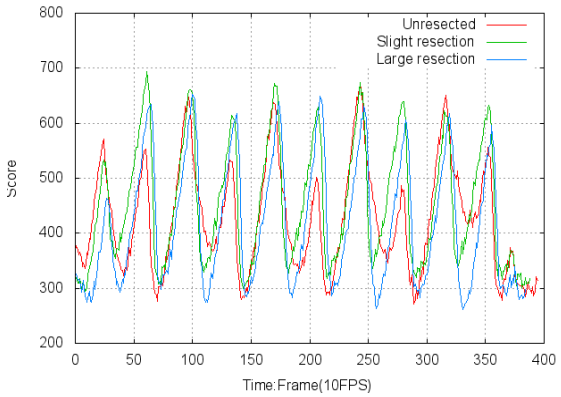

Fig. 12. When the virtual camera is rotated +10 degrees around the X axis relative to the real camera, the score changes when it moves back and forth ±30 mm in the Y axis direction on the velocity 10 mm/sec.

4) Change in camera coordinates in virtual space angle around X-axis +10 degrees, Y-axis ±30 mm, 5 sets

The angle of the camera in the virtual space is changed to +10 degrees, and the instructions are not changed.

The graph is shown in Fig. 13. The worst score is for the liver model that has not been respected, and the matching rate is low. The score fluctuates more for the liver model with less resection than for the liver model with more resection. The score value is lower, the fluctuation range is smaller, and the matching rate is higher for the liver model with more resection.

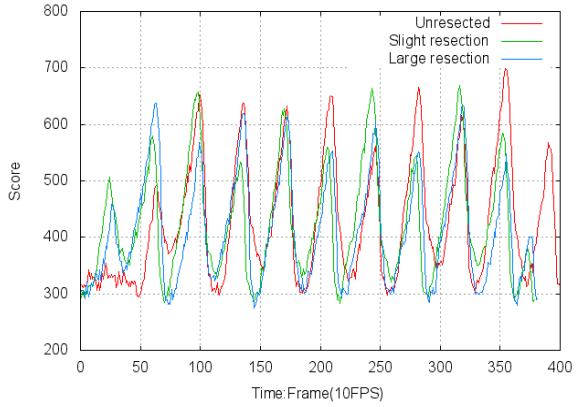

Fig. 13. When the virtual camera is rotated −10 degrees around the X axis relative to the real camera, the score changes when it moves back and forth ±30 mm in the Y axis direction on the velocity 10 mm/sec.

B. Y-axis Rotation Errors

Fig. 14 shows a graph obtained in virtual space without moving the camera's coordinates. Compared to movement along the X axis (Fig. 9), tracking accuracy is generally lower for movement along the Y axis (Fig. 14). This is because the amount of change in organ geometry is significantly less.

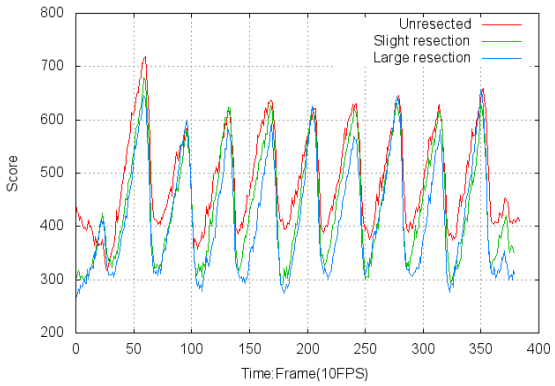

Fig. 14. The score changes when it moves back and forth ±30 mm in the Y axis direction on the velocity 10 mm/sec.

1) Change in camera coordinates in virtual space angle around Y-axis +10 degrees, X-axis ±30 mm, 5 sets

The angle of the camera in the virtual space was changed to +10 degrees around the Y-axis, and the instruction to move the parallel translation was moved at a speed of 30mm per second in the X-axis direction. The graph is shown in Fig. 15; the overall agreement is good because the X-axis migration has a lower overall score and less vertical variation. The highest scores are for the liver model with resection and the lowest scores are for the liver model without resection.

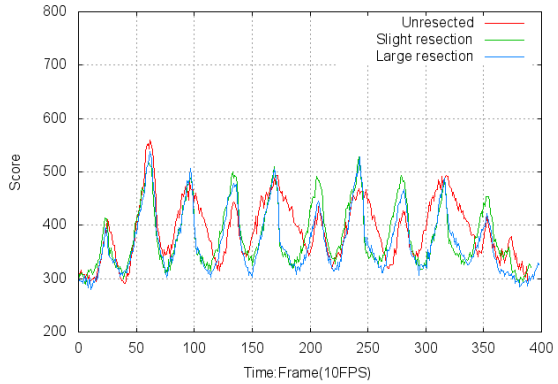

Fig. 15. When the virtual camera is rotated +10 degrees around the Y axis relative to the real camera, the score changes when it moves back and forth ±30 mm in the X axis direction on the velocity 10 mm/sec.

2) Change in camera coordinates in virtual space angle around Y-axis −10 degrees, X-axis ±30 mm, 5 sets

The results of evaluating the tracking accuracy of the liver by changing the angle of the camera in the virtual space by −10 degrees around the Y-axis are shown in Fig. 16. This was also an X-axis shift, with generally good scores and little variation in that. The liver model with hepatic resection had relatively good scores. The liver models without hepatic resection showed relatively poor matching rates.

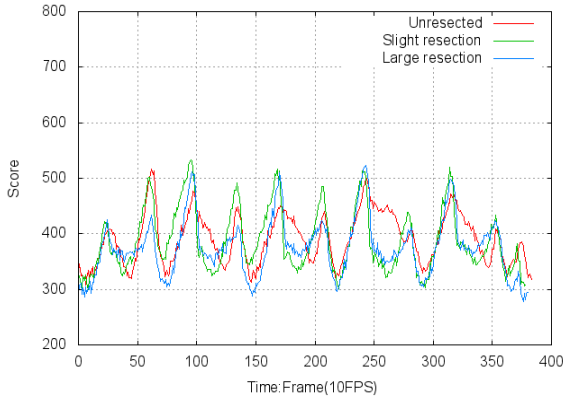

Fig. 16. When the virtual camera is rotated −10 degrees around the Y axis relative to the real camera, the score changes when it moves back and forth ±30 mm in the X axis direction on the velocity 10 mm/sec.

3) Change in camera coordinates in virtual space angle around Y-axis +10 degrees, Y-axis ±30 mm, 5 sets

The angle of the camera in the virtual space was changed to +10 degrees around Y-axis, and the parallel rotation measurement device was moved at a speed of 30mm per second in the Y-axis direction to take pictures and evaluate the tracking accuracy of the liver. This is shown in Fig. 17. Overall, the three liver models scored slightly better than without error because of error. The worst scoring liver model was the non-ablated liver model, and the best scoring liver model was the heavily ablated liver model.

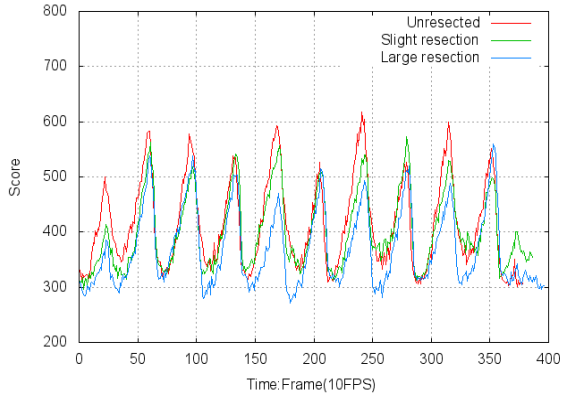

Fig. 17. When the virtual camera is rotated +10 degrees around the Y axis relative to the real camera, the score changes when it moves back and forth ±30 mm in the Y axis direction on the velocity 10 mm/sec.

4) Change in camera coordinates in virtual space angle around Y-axis −10 degrees, Y-axis ±30 mm, 5 sets

The angle of the camera in the virtual space was changed to −10 degrees around the Y-axis, and the tracking accuracy of the liver was evaluated without changing the command of the parallel rotation measurement device. The graph is shown in Fig. 18: despite the Y-axis shift, the scores and their variability did not deteriorate that much. This seems to be due to the positive effect of the error. The difference between the three liver shapes is also small. This case needs further investigation.

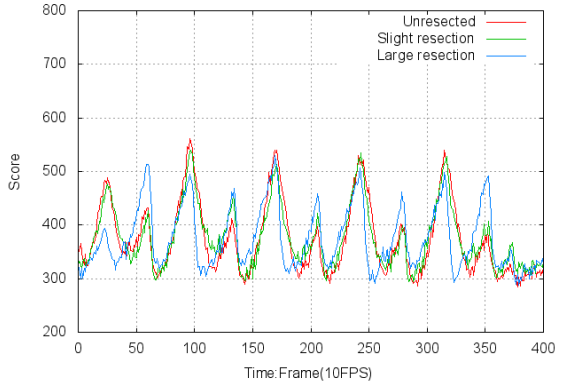

Fig. 18. When the virtual camera is rotated −10 degrees around the Y axis relative to the real camera, the score changes when it moves back and forth ±30 mm in the Y axis direction on the velocity 10 mm/sec.

IV. Conclusion

The tracking accuracy for movement in the X-axis direction is higher than that for movement in the Y-axis direction. This is because the DDM follows changes in the depth direction to search for organs, so it is preferable to have a larger amount of deformation in depth. In the case of movement in the X-axis direction, the tracking accuracy is already good when there is no error, so the effect of the error will vary from case to case. On the other hand, in the case of movement in the Y-axis direction, when there is no error, i.e. when the amount of change in the depth image is small, the amount of change in the depth image increases when there is an error, and the tracking accuracy always improves.

From the above, the organ tracking algorithm is functioning properly with an error of 0.037 mm excluding a few millimeters of the Kinect v2's depth error. DDM improves the accuracy of organ tracking for the following reasons:

(1) The shape of the organ becomes complex due to surgical manipulation.

(2) The difference between the real coordinates and the camera coordinates occurs due to the attachment of the depth camera.

In the future, we plan to add a function that realistically transfers the deformation of the real organ to the virtual organ.

Conflict of Interset

The authors declare no conflict of interest.

Author Contributions

Miho Asano, Tsuneo Jozen, Kaoru Watanabe, and Hiroshi Noborio contributed to the research concept and design; Miho Asano, Satoshi Numata, Kaoru Watanabe, and Hiroshi Noborio conceived the project and the study hypothesis; Miho Asano, Kaoru Watanabe, and Hiroshi Noborio designed and participated in performing the experiments; Miho Asano, Satoshi Numata, and Hiroshi

Noborio tested the software, analyzed the data; Miho Asano, Satoshi Numata, and Kaoru Watanabe executed implementation and evaluation of programming; Miho Asano analyzed the data; Miho Asano and Hiroshi Noborio clearly wrote the paper by manuscript rewriting; all authors have approved the final version.

ACKNOWLEDGMENT

The authors wish to thank undergraduate students Takumi Hirakawa and Ryo Miyazaki for his experimental efforts. This study was supported partly by 2014 Grants-in-Aid for Scientific Research (No. 26289069) from the Ministry of Education, Culture, Sports, Science, and Technology. Further support was provided by the 2014 Cooperation Research Fund from the Graduate School at Osaka Electro-Communication University.

REFERENCES

[1] Wikipedia. Plastic survey. [Online]. Available: https://en.wikipedia.org/wiki/Plastic_surgery
[2] A. DiGioia, B. Jaramaz, F. Picard, and L. P. Nolte, *Computer and Robotic Assisted Hip and Knee Surgery*, New York: Oxford University Press, 2004.
[3] Wikipedia. Neuronavigation. [Online]. Available: https://en.wikipedia.org/wiki/Neuronavigation
[4] Wikipedia. 3D_stereo_view. [Online]. Available: https://en.wikipedia.org/wiki/3D_stereo_view
[5] Wikipedia. Simultaneous_localization_and_mapping. [Online]. Available: https://en.wikipedia.org/wiki/Simultaneous_localizationand_mapping
[6] R. C. Smith and P. Cheeseman, "On the representation and estimation of spatial uncertainty," *The International Journal of Robotics Research*, vol. 5, no. 4, pp. 56–68, 1986.
[7] J. J. Leonard and H. F. D. Whyte, "Simultaneous map building and localization for an autonomous mobile robot," in *Proc. IROS'91 IEEE/RSJ International Workshop*, Osaka, 1991, pp. 1442–1447.
[8] A. J. Golby, *Image-Guided Neurosurgery*, Academic Press, 2015.
[9] S. Pieper, M. Halle, and R. Kikinis, "3D slicer," in *Proc. the 1st IEEE International Symposium on Biomedical Imaging: From Nano to Macro*, Arlington, 2004, pp. 632–635.
[10] R. Smith and P. Cheeseman, "On the representation and estimation of spatial uncertainty," *Int. J. Robotics Research*, vol. 5, no. 4, pp. 56–68, 1986.
[11] R. A. Brooks, "Visual map making for a mobile robot," in *Proc. IEEE Int. Conf. Robotics and Automation*, St. Louis, 1985, pp. 824–829.
[12] R. Chatila and J. P. Laumond, "Position referencing and consistent world modeling for mobile robots," in *Proc. IEEE Int. Conf. Robotics and Automation*, St. Louis, 1985, pp. 138–145.
[13] R. M. Artal and J. D. Tardós, "ORB-SLAM2: An open-source SLAM system for monocular, stereo and RGB-D cameras," *IEEE Transactions on Robotics*, vol. 33, no. 5, pp. 1255–1262, 2017.
[14] K. Konolige and G. R. Bradski, "An efficient alternative to SIFT or SURF," in *Proc. the 2011 International Conference on Computer Vision*, 2011, pp. 2564–2571.
[15] M. Koeda, S. Nishimoto, H. Noborio, and K. Watanabe, "Proposal and evaluation of AR-based microscopic brain surgery support system," in *Human-Computer Interaction. Recognition and Interaction Technologies*, M. Kurosu, Ed., Orlando: Springer, 2019, pp. 438–446.
[16] Wikipedia. Iterative_closest_point. [Online]. Available: https://en.wikipedia.org/wiki/Iterative_closest_point
[17] Y. Chen and M. Gerard, "Object modelling by registration of multiple range images," *Image Vision Comput.*, vol. 10, no. 3, pp. 145–155, 1991.
[18] P. J. Besl and N. D. McKay, "A method for registration of 3-D shapes," *IEEE Trans. Pattern Anal. Mach. Intell.*, vol. 14, no. 2, pp. 239–256, 1992.
[19] Z. Zhang, "Iterative point matching for registration of free-form surfaces," *Int. Journal of Computer Vision*, vol. 13, no. 2, pp. 119–152, 1994.
[20] S. Granger and X. Pennec, "Multi-scale EM-ICP: A fast and robust approach for surface registration," in *Proc. 7th European Conference on Computer Vision*, 2002, pp. 69–73.
[21] Y. Liu, "Automatic registration of overlapping 3D point clouds using closest points," *Journal of Image and Vision Computing*, vol. 24, no. 7, pp. 762–778, 2006.
[22] J. Salvi, C. Matabosch, D. Fofi, and J. Forest, "A review of recent range image registration methods with accuracy evaluation," *Journal of Image and Vision Computing*, vol. 25, no. 5, pp. 578–596, 2007.
[23] R. B. Rusu and S. Cousins, "3D is here: Point Cloud Library (PCL)," in *Proc. IEEE Int. Conf. Robotics and Automation*, 2011, pp. 1–4.
[24] Y. F. Wu, W. Wang, K. Q. Lu, Y. D. Wei, and Z. C. Chen, "A new method for registration of 3D point sets with low overlapping ratios," in *Proc. 13th CIRP conference on Computer Aided Tolerancing*, 2015, pp. 202–206.
[25] H. Noborio, K. Onishi, M. Koeda, *et al.*, "Motion transcription algorithm by matching corresponding depth image and Z-buffer," in *Proc. the 10th Anniversary Asian Conference on Computer Aided Surgery*, Kyusyu University, Fukuoka, Japan, 2014, pp. 60–61.
[26] H. Noborio, K. Watanabe, M. Yagi, *et al.*, "Image-based initial position/orientation adjustment system between real and virtual livers," *Jurnal Teknologi: Medical Engineering*, vol. 77, no. 6, pp. 41–45, 2015.
[27] K. Watanabe, M. Yagi, K. Ota, *et al.*, "Parameter identification of depth-depth-matching algorithm for liver following," *Jurnal Teknologi: Medical Engineering*, vol. 77, no. 6, pp. 35–39, 2015.
[28] K. Watanabe, M. Yagi, A. Shintani, *et al.*, "A new 2D depth-depth matching algorithm whose translation and rotation freedoms are separated," in *Proc. of the International Conference on Intelligent Informatics and Biomedical Sciences (ICIIBMS2015), Track 3: Bioinformatics, Medical Imaging and Neuroscience*, Okinawa, Japan, 2015, pp. 271–278.
[29] H. Noborio, K. Watanabe, M. Yagi, *et al.*, "Experimental results of 2D depth-depth matching algorithm based on depth camera Kinect v1," *Journal of Bioinformatics and Neuroscience*, vol. 1, no. 1, pp. 38–44, 2015.
[30] H. Noborio, K. Watanabe, M. Yagi, *et al.*, "Tracking a real liver using a virtual liver and an experimental evaluation with Kinect v2," in *Proc. of the 4th International Work-Conference on Bioinformatics and Biomedical Engineering*, Granada, Spain, 2016, pp. 149–162.
[31] K. Watanabe, M. Yagi, K. Onishi, M. Koeda, H. Noborio, and M. Kaibori, "Evaluation of depth-depth matching algorithm for following human liver whose motion is practical and also is occluded by human body," in *Proc. of the 10th MedViz Conference and the 6th Eurographics Workshop on Visual Computing for Biology and Medicine*, Bergen, Norway, 2016, pp. 135–138.
[32] M. Asano, T. Kuroda, S. Numata, T. Jozen, T. Yoshikawa, and H. Noborio, "Convergence stability of depth-depth-matching-based steepest descent method in simulated liver surgery," *International Journal of Pharma Medicine and Biological Sciences*, vol. 10, no. 2, pp. 60–67, April 2021. doi: 10.18178/ijpmbs.10.2.60-67
[33] M. Asano, T. Kuroda, S. Numata, T. Jozen, T. Yoshikawa, and H. Noborio, "Stability maintenance of depth-depth matching of steepest descent method using an incision shape of an occluded organ," in *Human-Computer Interaction. Human Values and Quality of Life*, M. Kurosu, Ed., Springer, 2020, pp. 539–555.
[34] H. Noborio, S. Yoshida, K. Watanabe, D. Yano, and M. Koeda, "Comparative study of depth-image matching with steepest descendent and simulated annealing algorithms," in *Proc. of the 11th International Joint Conference on Biomedical Engineering Systems and Technologies*, 2018, pp. 77–87.
[35] S. Numata, M. Koeda, K. Onishi, K. Watanabe, and H. Noborio, "Performance and accuracy analysis of 3D model tracking for liver surgery," in *Human-Computer Interaction. Recognition and Interaction Technologies*, M. Kurosu, Ed., Springer, 2019, pp. 524–533.

[36] H. Noborio, K. Onishi, M. Koeda, K. Watanabe, and M. Asano, "Depth–Depth matching of virtual and real images for a surgical navigation system," *International Journal of Pharma Medicine and Biological Sciences*, vol. 10, no. 2, pp. 40–48, April 2021.
[37] M. Asano, Y. Yamada, T. Kunii, M. Koeda, and H. Noborio, "Use of mixed reality in attachment of surgical site measurement robot to surgical bed," *Journal of Robotics and Mechatronics*, vol. 36, no. 3, pp. 694–703, 2024.